



Cite this: *Nanoscale*, 2016, **8**, 17085

Received 22nd July 2016,
 Accepted 27th August 2016

DOI: 10.1039/c6nr05781k

www.rsc.org/nanoscale

Superparamagnetic anisotropic nano-assemblies with longer blood circulation *in vivo*: a highly efficient drug delivery carrier for leukemia therapy†

Fei Xiong,^{*a} Jilai Tian,^a Ke Hu,^a Xiawen Zheng,^a Jianfei Sun,^a Caiyun Yan,^b Juan Yao,^b Lina Song,^a Yu Zhang^a and Ning Gu^{*a}

Leukemia, unlike solid tumors, has no definite shape and spreads throughout the whole circulatory system, therefore the therapy of leukemia requires medication to stay longer in the circulatory system. Anisotropic nanoparticles, showing longer blood circulating life than that of isotropic nanoparticles reported in previous research, meet the demands of leukemia therapy. Based on this strategy, superparamagnetic anisotropic nano-assemblies (SANs) were fabricated and loaded with vincristine (VCR) to form VCR-SANs. When compared to the same dose of VCR-loaded isotropic nano-assemblies (SINs), the decrease in the leukocytes count and the positive expression ratio of CD13 in the VCR-SANs group were 19.38% and 16.4%, respectively, which indicated the improved anti-leukemia activity of the VCR-SANs. From the results of the pharmacokinetics study, the VCR-SANs remarkably held the amount of drug removed from the whole body per unit time half of the isotropic group and the concentration of drug in blood plasma against time was 2.1 times the isotropic group, demonstrating the rapid and sustained release behavior and longer blood circulation when combined with the results of *in vivo* tissue distribution studies. In summary, anisotropic nano-assemblies were found to be more promising than isotropic nano-assemblies *via* our *in vivo* and *in vitro* examinations.

Nanoparticles-mediated drug delivery is potentially changing the way we treat diseases. It not only improves drug delivery and release, but also prolongs the circulation time, enhances cellular uptake and strengthens the therapeutic efficiency, making remarkable progress over single-drug approaches. Typically, single spheres and surface engineered nanoparticles have been used in the localized targeted delivery of drugs. However, most of the current nano-carrier research has

focused on developing efficient local drug delivery for solid tumors. Nanomaterials developed for the treatment of liquid tumors have seldomly been studied and typical spherical nano-carriers relying on the enhanced permeability and retention effect (EPR) may not be suitable for non-solid tumors, like leukemia.

Leukemia is a cancerous disease that affects the blood-forming cells in the body. It occurs more commonly in developed countries and is the most common type of cancer found in children. Significant research into the causes, prevalence, diagnosis, treatment and prognosis of leukemia has been performed, while the exact cause of leukemia is unknown, and there is still no proven effective therapy. Unlike solid tumors, leukemia has no definite shape and EPR-mediated tumor accumulation does not have much meaning to the therapy of leukemia. Based on the specificity of liquid tumors, the therapeutic strategy of leukemia lies with a particular emphasis on prolonging the action time of a drug in the circulatory system. Nanomaterials with a long hematogenous circulation serving as drug carriers may be a good solution.

Research has shown that the circulation time of anisotropic nanomaterials is significantly longer than isotropic control samples. Much of the previous research has examined elongated particles, which were found to have increased circulation times with respect to their spherical counterparts, though this effect was attributed to the size and shape of the particles as well as their deformability.¹ In addition, another study on nanostructure shape also mentioned that the particle shape and degree of flexibility influenced the entry and passage of drug carriers.² Reports have shown that elliptic nanoparticles under various blood flow conditions possess greater adhesion properties than circular particles, which gives rise to long circulating times.³ Other investigations suggest that filamentous micelles do not accumulate in the spleen due to their unique shape,⁴ and the elastic deformation of particles was found to affect their cellular interactions, circulating time and biodistribution.^{1,5-7} According to these works, we believe that nanomaterials with an analogous anisotropic shape will

^aState Key Laboratory of Bioelectronics, Jiangsu Laboratory for Biomaterials and Devices, School of Biological Science and Medical Engineering, Southeast University, Nanjing 210096, China. E-mail: xiongfei@seu.edu.cn, guning@seu.edu.cn

^bChina Pharmaceutical University, Nanjing, Jiangsu, 210009, China

† Electronic supplementary information (ESI) available: Experiments, Fig. S1 and S2. See DOI: 10.1039/c6nr05781k

have advantages as drug-carriers aimed at the treatment of non-solid tumors *in vivo* when compared with isotropic nanomaterials.

Herein, we fabricated novel superparamagnetic anisotropic nano-assemblies (SANs) carrying hydrophobic anticancer drugs against leukemia. The SANs were prepared by combining solvent-exchange and static magnetic field assisted assemblies. Vincristine (VCR, a key agent for the treatment of leukemia)^{8,9} was loaded on the oleic acid (OA) layer of the SANs for their evaluation as a drug carrier. The characterization results showed that the performance of the VCR-SANs as drug carriers was as good as a VCR-loaded superparamagnetic isotropic nano-assembly's (VCR-SINs) control sample *in vitro*, but the results obtained for leukemia therapy demonstrated that the VCR-SANs prevail over the VCR-SINs *in vivo*. In addition, the results of cellular uptake *in vitro*, pharmacokinetics and biodistribution *in vivo* also demonstrated the biological priority of the SANs, which was derived from the anisotropy of the carriers.

The strategy of fabricating VCR-SANs combining the phase transfer of magnetic nanoparticles and magnetic drive assembly is shown schematically in Scheme 1.

Oleic acid coated iron oxide nanoparticles ($\text{Fe}_3\text{O}_4\text{@OA}$) dispersed in THF were mixed with VCR, surfactant (Pluronic 188, poly(ethylene oxide)–poly(propylene oxide)tri-block copolymer) and then doubly distilled water. After ultrasonic dispersion, the whole mixture was placed in a static magnetic field. When the magnetic field was applied, the monodispersed $\text{Fe}_3\text{O}_4\text{@OA}$ nanoparticles formed anisotropic magnetic colloidal assemblies parallel to the applied magnetic field. Hydrophobic interactions between the neighboring $\text{Fe}_3\text{O}_4\text{@OA}$ nanoparticles caused by the OA layers maintained the anisotropic structure of the SANs when the external magnetic field was removed. VCR was loaded on the OA layer *via* hydrophobic interactions and the monodispersed $\text{Fe}_3\text{O}_4\text{@OA}$ nanoparticles provided a fixed surface dimension for stable drug-loading efficiency. The pluronic coating prevents aggregation and

ensures the stability of VCR-SANs. VCR was also loaded onto SINs, which were prepared using a similar method to that used for the VCR-SANs, only the magnetic field was neglected.

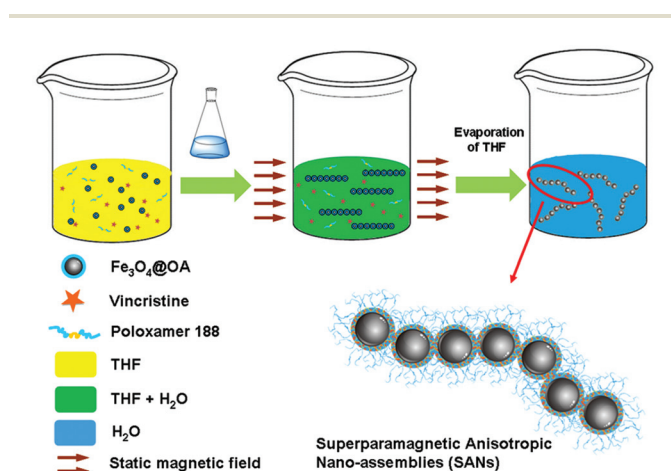
The $\text{Fe}_3\text{O}_4\text{@OA}$ nanoparticles used to fabricate the VCR-SANs and VCR-SINs were with good monodispersity and the TEM size was 9.81 ± 1.02 nm (Fig. 1a). Since both nano-assemblies comprised of these nanoparticles as building blocks, the hydrodynamic diameter (58.15 ± 4.12 nm and 53.17 ± 3.24 nm) and zeta potentials (-37.6 mV and -35.3 mV) were not significantly different between VCR-SANs and VCR-SINs. However, the TEM images showed that the morphology of VCR-SANs and VCR-SINs were evidently different (Fig. 1a and b). Based on the statistical data, the difference can be expressed by the anisotropic degree, which was calculated according to the following equation.

$$e = L/D$$

where L is the length and D is the diameter of the nano-assemblies. The anisotropic degree of the VCR-SANs was calculated to be 9.64 ± 5.45 , whereas the anisotropic degree of the VCR-SINs was just 1.07 ± 0.04 .

The stabilities of the two nano-assemblies were further examined *via* comparing the hydrodynamic diameter and zeta potential months after their preparation. The appearance of the two nano-assemblies were transparent after 3 months meanwhile the diameter (59.19 ± 6.39 nm and 55.21 ± 5.54 nm) and the zeta potential (-35.9 mV and -34.1 mV) showed small changes from the freshly prepared samples, indicating that the two nano-assemblies were stable at room temperature for 3 months.

Although the drug is not chemically conjugated to the nano-assemblies, strong hydrophobic interactions of the internal OA layer of $\text{Fe}_3\text{O}_4\text{@OA}$ nanoparticles trap the drug within the assemblies. The external surfaces of the nano-assemblies exposed to the systematic circulation environment display faster drug release, while the internal adjacent surface hidden from the release medium show slower drug release. The drug encapsulation efficiencies (91.29% and 93.75%) of the VCR-SANs and VCR-SINs show no significant differences. The release rate of VCR solution group was fast with a cumulative release nearly up to 90% after the first 2 h, while it was after about 6 h in the VCR-SANs ($88.8 \pm 3.4\%$) and VCR-SINs ($88.1 \pm 3.5\%$) groups (Fig. 2). These results illustrated that both VCR-SANs and VCR-SINs showed a similar sustained



Scheme 1 The fabrication process and ideal structure of the vincristine-loaded superparamagnetic anisotropic nano-assemblies (VCR-SANs).

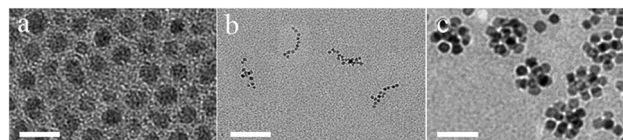


Fig. 1 Transmission electron microscopy (TEM) images of (a) $\text{Fe}_3\text{O}_4\text{@OA}$ dispersed in *n*-hexane (scale bar = 20 nm), (b) VCR-SANs (scale bar = 100 nm) and (c) VCR-SINs (scale bar = 50 nm) dispersed in water.

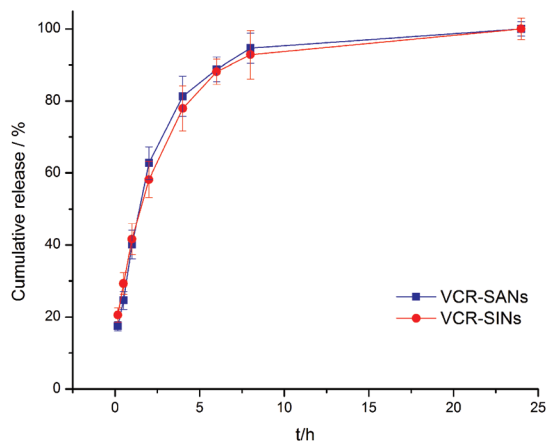


Fig. 2 The cumulative release curves obtained for VCR-SANs and VCR-SINs.

release of VCR *in vitro* due to the OA layer and copolymer encapsulation.

According to all the characterization results, we can conclude that the main difference between the VCR-SANs and VCR-SINs is the degree of anisotropy. The difference in the degree of anisotropy makes the anisotropic materials perform better in the treatment of leukemia on account of the prolonged blood circulation time. To investigate the anti-cancer effects of VCR-SANs, a leukemia animal model was set up by inoculation with K562 cells. During the third week after inoculation, some phenomena were found in mice, like decreased ambulation, reduced body weight and ruffled hair. Leukemia cells were found on the peripheral blood smears using Wright's stain (Fig. S1a†), and the count of peripheral blood leukocyte was 5 times as much as that obtained before inoculation (Fig. S1b†). Moreover, CD13 in peripheral blood was detected and the positive expression ratio of SSC (side scatter) and FSC (forward scatter) were 31.48% and 29.56%, respectively (Fig. S1c†). All of these results confirmed that the leukemia model was a success. Then, these leukemia-bearing mice were injected with the different VCR delivery systems.

Changes in the number of leukocytes and positive expression ratios of CD13 in peripheral blood one week after administration are displayed in Fig. 3a and b, which show that different degrees of anisotropy in the nano-assemblies showed different therapeutic efficiencies: the leukocytes count in the VCR-SANs group decreased by 19.38% and the positive expression ratio of CD13 in the VCR-SANs group decreased by 16.42% when compared with the VCR-SINs group. In addition, when compared to the VCR control group, the data showed larger differences with decreases of 32.47% and 36.17%. All of these significant differences of changes in the number of leukocytes and variation of the positive expression of CD13 in peripheral blood *in vivo*, compared to VCR and VCR-SINs, VCR-SANs brought the unique performance by playing its own role of chain-like.

To investigate the *in vivo* basis of the increased anti-leukemia effectiveness, we determined the dynamic behavior of VCR-SINs and VCR-SANs in the systemic circulatory system and tissues, respectively. After intravenous administration of a single dose of 6 mg kg^{-1} , the VCR concentration in plasma and tissues at various times were determined by HPLC (Fig. 4)

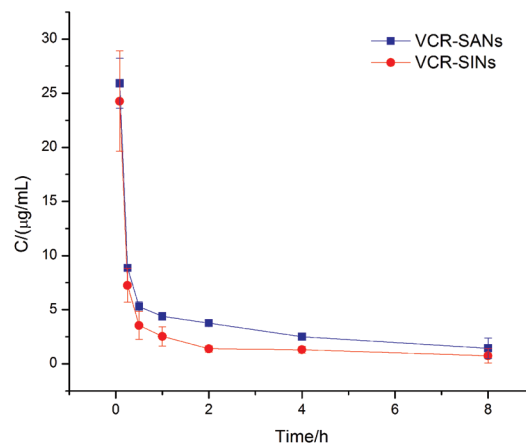


Fig. 4 The plasma concentration-time curve obtained for VCR with different delivery systems in rats after intravenous administration at a single identical dose of 6 mg kg^{-1} ($n = 3$).

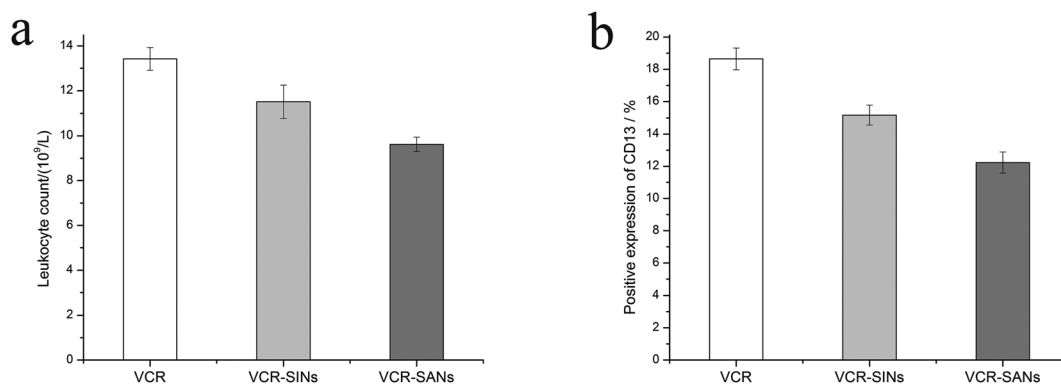


Fig. 3 Anti-leukemia effects of VCR, VCR-SINs and VCR-SANs. (a) Changes in the number of leukocytes in peripheral blood after administration via the tail vein for one week ($*p < 0.05$ vs. VCR-SINs group). (b) Variation of the positive expression of CD13 in peripheral blood after administration via the tail vein for one week ($*p < 0.05$ vs. VCR-SINs group).

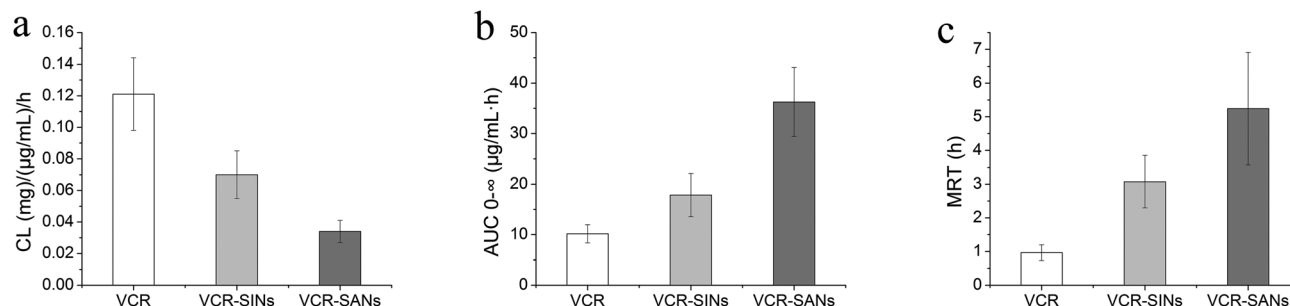


Fig. 5 The main pharmacokinetics parameters obtained for VCR with the different delivery systems in rats after intravenous administration at a single identical dose of 6 mg kg^{-1} ($n = 3$): (a) Total body clearance (CL), (b) the area under the plasma concentration-time curve ($\text{AUC}_{0-\infty}$) and (c) mean residence time (MRT) ($*p < 0.05$ vs. VCR, $\#p < 0.05$ vs. VCR-SINs).

and data analysis performed using PKSolver software.¹⁰ Some typical parameters, including the area under the plasma concentration-time curve from 0 to infinite time ($\text{AUC}_{0-\infty}$), total body clearance (CL) and mean residence time (MRT) are reported in Fig. 5. The VCR-SANs group showed 2.1 and 1.7 times the $\text{AUC}_{0-\infty}$ and MRT of the VCR-SINs group, respectively, which indicated more amount of drug as well as a longer residence time in the circulating system, therefore VCR-SANs had better therapeutic effects for blood diseases. The CL decreased by 48.6% in the VCR-SANs group when compared to the group of VCR-SINs. CL is the only parameter that can correctly estimate the speed of drug clearance in the body and reflects the capacity of drug elimination in an organ, particularly the liver and kidney. Lower value of CL indicates fewer particles eliminated, which further proves the long

circulating time of the SANs, and consequently, facilitates the treatment of leukemia.

The study of tissue distribution was further conducted using tissue biopsies, including the heart, liver, spleen, lung, and kidneys. Carriers that contained iron could react to prussian blue, and the area of blue could reflect the degree of iron uptake. From Fig. 6, we can see that the VCR-SINs are prone to be arrested in the liver and spleen, but few blue spots are found in the VCR-SANs group, which may be the reason for the difficult engulfment of the chain-like carriers under blood flow. It was found that VCR-SANs preferred to circulate in the blood stream with less capability of initiating phagocytosis than that of the VCR-SINs, which entailed the lower distribution in liver and spleen in the VCR-SANs group.

To preliminarily evaluate the safety of SANs, the sectioned organs were proceeded further for histological evaluation with hematoxylin and eosin (HE) staining. The results are displayed in Fig. S2,[†] from which can be seen all tissues were with full round cells and almost no inflammation or necrosis was observed, which preliminary demonstrates the low toxicity of SANs.

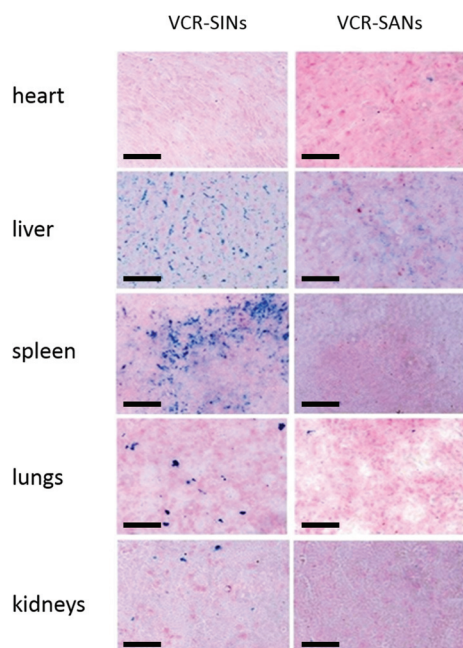


Fig. 6 Prussian blue staining of the heart, liver, spleen, lung and kidneys of mice after intravenous injection at an identical dose of 10 mg kg^{-1} for the same time, observed at $\times 400$ (scale bar = $100 \mu\text{m}$).

Conclusions

In summary, a simple solvent-exchange and magnetic drive assembly method was developed to form superparamagnetic anisotropic nano-assemblies (SANs) within the oleic acid layer and the hydrophobic anticancer VCR-loaded agents. When compared with the same drug dose of isotropic nano-assemblies, the VCR-loaded superparamagnetic anisotropic nano-assemblies were more effective in treating leukemia. The results of the cells' experiments demonstrated the great anti-leukemia capability of the VCR-SANs and the pharmacokinetics experiments, together with the tissue distribution experiments, notably suggested that the anisotropic nano-assemblies were retained in the circulatory system for longer. In conclusion, the superparamagnetic anisotropic nano-assemblies will have the potential to realize high therapeutic efficiency for leukemia treatment in further pre-clinical and clinical studies. In addition, this work and effort may greatly

expedite the use of drug carriers in the treatment of diseases of the hematopoietic and lymphoid tissues, and solid tumors, which require longer circulation time.

Acknowledgements

This work was financially supported by the National Natural Science Foundation of China (81473160), the Basic Research Program of Jiangsu Province (Natural Science Foundation, no. BK20151422), Fundamental Research Funds for the Central Universities (2242014R30013 and 2242016K40033), the National High Technology Research and Development Program of China (no. 2013AA032205) and the Qing Lan Project.

Notes and references

- 2 S. Venkataraman, J. L. Hedrick, Z. Y. Ong, C. Yang, P. L. R. Ee, P. T. Hammond and Y. Y. Yang, *Adv. Drug Delivery Rev.*, 2011, **63**, 1228.
- 3 K. Müller, D. A. Fedosov and G. Gompper, *Sci. Rep.*, 2014, **4**, 4871.
- 4 Y. Geng, P. Dalhaimer, S. Cai, R. Tsai, M. Tewari, T. Minko, M. Tewari, T. Minko and D. E. Discher, *Nat. Nanotechnol.*, 2007, **2**, 249.
- 5 J. P. Best, Y. Yan and F. Caruso, *Adv. Healthcare Mater.*, 2012, **1**, 35.
- 6 X. Yi, X. Shi and H. Gao, *Phys. Rev. Lett.*, 2011, **107**, 098101.
- 7 G. R. Hendrickson and L. A. Lyon, *Angew. Chem., Int. Ed.*, 2010, **49**, 2193.
- 8 S. O'Brien, G. Schiller, J. Lister, L. Damon, S. Goldberg, W. Aulitzky, D. Ben-Yehuda, W. Stock, S. Coutre, D. Douer, L. T. Heffner, M. Larson, K. Seiter, S. Smith, S. Assouline, P. Kuriakose, L. Maness, A. Nagler, J. Rowe, M. Schaich, O. Shpilberg, K. Yee, G. Schmieder, J. A. Silverman, D. Thomas, S. R. Deitcher and H. Kantarjian, *Clin. Oncol.*, 2013, **31**, 676.
- 9 J. A. Silverman and S. R. Deitcher, *Cancer Chemother. Pharmacol.*, 2013, **71**, 555.
- 10 Y. Zhang, M. R. Huo and J. P. Zhou, *Comput. Methods Progr. Biomed.*, 2010, **99**, 306.

- 1 T. J. Merkel, K. P. Herlihy, S. W. Jones, F. R. Kersey, A. R. Shields, M. Napier, J. C. Luft, H. Wu, W. C. Zamboni, A. Z. Wang, J. E. Bear and J. M. DeSimone, *Proc. Natl. Acad. Sci. U. S. A.*, 2011, **108**, 586.